Inversion of Dynamic Production Data for Permeability: Fast Streamline-Based Computation of Sensitivity Coefficients of Fractional Flow Rate

Xian-Huan Wen*, Clayton V. Deutsch†, and A. S. Cullick‡

Abstract

Generation of permeability field in a reservoir model that matchs historical dynamic production data requires an inverse calculation. A gradient method is typically used to solve the inverse minimization problem and requires sensitivity coefficients of reservoir responses, e.g. fractional flow rate or pressure, with respect to the change in the permeability. This paper presents a novel semi-analytical streamline-based method for computing such sensitivity coefficients under the framework of two-phase (oil-water) flow conditions. This method

*Corresponding author, Chevrontexaco Exploration and Production Technology Company, San Ramon, California, USA. e-mail: xwen@chevrontexaco.com, Fax: 1-925-842 6283

†Department of Civil & Environmental Engineering, University of Alberta, Canada.

‡Landmark Graphics, Austin, Texas, USA.

is shown to be significantly faster and generate permeability fields with lower objective function than the traditional perturbation method. The method decomposes the multiple-dimensional full flow problem into multiple 1D problems along streamlines. The sensitivity of fractional flow rate at the production well is directly related to the sensitivity of time-of-flight (TOF) along each individual streamline and the sensitivity of pressure at grid cells along the streamline. The sensitivity of TOF of a streamline can be obtained analytically. The sensitivity of pressure is obtained as part of a fast single phase flow simulation. The proposed method is implemented in a geostatistically-based inverse technique, called the sequential self-calibration (SSC) method. Results for fractional flow rate sensitivities are presented and compared with the traditional perturbation method. This new method can be easily extended to compute sensitivity coefficients of saturation (concentration) data.

Key Words: Inverse Problem, Sequential-Self Calibration Method, Master Point, Spatial Correlation, Perturbation, Two-phase Flow, Streamline Simulation.

1 Problem Statement

Accurate reservoir simulation and performance forecasting call for realistic geological reservoir models that are consistent with all relevant data, including static data (conceptual geological data, well log and core data, and seismic data) and dynamic data (well test data, pressure data from permanent gauges, historical fractional flow rate data, and saturation data). Geostatistical techniques have proved to be powerful tools for constructing such complex geological reservoir models providing an assessment of related uncertainty (Journel, 1989; Deutsch and Journel, 1998). Honoring both hard and soft static data is performed through well established co-simulation techniques (e.g., Xu et al., 1992; Zhu and Journel, 1993; Gómez-Hernández and Journel, 1993). However, honoring dynamic data simultaneously remains a challenge and is a very active area of research (e.g., Oliver, 1996; He et al., 1996; Wen, 1996; Gómez-Hernández et al., 1997; Landa, 1997; Tjelmeland, 1997; Wen et al., 1998, 2000; Hu et al., 1999).

The main difficulty in honoring dynamic production data is the global and nonlinear relationship between dynamic data and reservoir petrophysical properties, e.g., porosity and permeability, through the flow equations. Matching dynamic production data in geostatistical reservoir models is an inverse parameter estimation problem in which flow equations must be solved to establish the relationship between data and model parameters (Tarantola, 1987; Sun, 1994). The inverse problem is often ill-posed with no unique solution.

A common way for solving an inverse problem is to pose it as an optimization (minimization) problem in which an objective function measuring the mismatch be-

tween observed data and model responses is minimized. The optimization method searches for optimal model parameters that best match the data, subject to constraints imposed by the flow equations and various spatial statistics. The gradient-based methods typically used to solve the optimization problem require calculating the sensitivity coefficients of the reservoir responses, e.g., pressure, saturation and fractional flow rate, with respect to the model parameters, e.g., porosity and permeability.

In this paper, we adapte an iterative geostatistically-based inverse technique, the sequential self-calibration (SSC) method, developed originally by Gómez-Hernández and co-workers (Gómez-Hernández et al., 1997). The SSC method has been shown to be flexible, robust and computationally efficient in honoring single phase dynamic pressure data from e.g., permanent pressure gauges, simultaneous multiple well interference tests, or early production data before water/gas breakthrough (Capilla et al., 1997; Wen et al., 1996, 1998, 1999). The unique aspects of the SSC method are (1) the concept of master points that reduces the parameter space to be estimated in the optimization, (2) a perturbation mechanism based on kriging that accounts for the spatial correlation of perturbations, and (3) a fast method for computing sensitivity coefficients that makes the inversion feasible. Readers are referred to the above references for detailed description of the SSC methodology.

In this paper, we present the SSC method for inverting two-phase fractional flow rate data, such as watercut (WCUT) or gas/oil ratio (GOR) at production wells, in addition to the pressure. For the case of tracer test in hydrogeology, fractional flow

rate data are equivalent to the tracer (cumulative) concentration at observation wells. The objective function to be minimized is of the following form:

$$O = \sum_{w_p=1}^{n_{wp}} \sum_{t_p=1}^{n_{tp}} W_p(w_p, t_p) \left[\widehat{p}(w_p, t_p) - p(w_p, t_p)\right]^2 + \sum_{w_f=1}^{n_{wf}} \sum_{t_f=1}^{n_{tf}} W_f(w_f, t_f) \left[\widehat{f}(w_f, t_f) - f(w_f, t_f)\right]^2 \tag{1}$$

where $\widehat{p}(w_p, t_p)$ and $p(w_p, t_p)$ are the observed and simulated pressure at well w_p at time t_p. $\widehat{f}(w_f, t_f)$ and $f(w_f, t_f)$ are the observed and simulated fractional flow rate at well w_f at time t_f. $W_p(w_p, t_p)$ and $W_f(w_f, t_f)$ are weights assigned to pressure and fractional flow rate data at different wells and at different time. n_{wp} and n_{wf} are the number of wells that have pressure and fractional flow data. n_{tp} and n_{tf} are the number of time steps for pressure and fractional flow measurements.

In order to find the optimal perturbations of permeability at master locations that minimize the objective function (1) using a gradient-based method, the sensitivity coefficients (derivatives) of pressure and fractional flow rate at the wells with respect to perturbations of permeability at all master points at all time steps are required, i.e.,

$$S_{p,j}(w_p, t_p) = \frac{\partial p(w_p, t_p)}{\partial \triangle k_j}, \quad \forall w_p, t_p, k_j \tag{2}$$

and

$$S_{f,j}(w_f, t_f) = \frac{\partial f(w_f, t_f)}{\partial \triangle k_j}, \quad \forall w_p, t_p, k_j \tag{3}$$

with $j = 1, ..., n_m$ being the index of master points.

A method for computing sensitivity of pressure at **all** locations ($S_{p,j}(x, t_p), x \in$ all cells, not limited to the well locations) within the flow simulation has been presented by Gómez-Hernández et al. (1997) and Wen et al. (1998). Here, we present the fast calculation of the sensitivity coefficient of fractional flow rate, $S_{f,j}(w_f, t_f)$.

Computing sensitivity coefficients of reservoir responses to reservoir petrophysical properties has been an active research topic for decades and many sophisticated methods have been developed in the literature. Most of these approaches fall into one of three categories: perturbation techniques, direct methods, and adjoint state methods. A review of methods for computing sensitivity coefficient is not the subject of this paper. Interested readers can refer to references (e.g., Yeh, 1986; Chu et al., 1995) for details. In this paper, we recall the simplest method, the perturbation method, which is also the most CPU time demanding method, nevertheless remains popular algorithm due to its simplicity and wide range applicability. We explain the shortcomings of the perturbation method and then present a novel and faster streamline-based semianalytical method.

The proposed method capitalizes on (1) the analytical 1D solutions of fractional flow rate along each streamline (Thiele et al., 1994; Batycky et al., 1997), (2) the capability of obtaining sensitivity coefficients of pressure over the entire field after solving single phase flow equations, and (3) the assumption that streamline geometry remains unchanged when perturbing permeabilities, the sensitivity coefficients of fractional flow rate are obtained extremely fast by simple book-keeping the stream-

line paths in space. In addition, the permeability perturbations are jointly considered rather than one at a time as in the perturbation method. This new method is then implemented within the SSC framework for generating geostatistical permeability realizations that simultaneously honor transient pressure and fractional flow rate data at producing wells. Streamlines are updated in each outer iteration of the SSC inversion, which, to some extent, self-corrects the assumption of fixed streamline geometry during the calculation of sensitivity coefficients. The assumption of streamline geometry remaining unchanged during the perturbation could be justified by comparing the SSC inverse results based on both the perturbation method and the proposed method. Finally the CPU advantage of the proposed method is demonstrated.

This paper is organized as follows. Traditional perturbation method of computing sensitivity coefficients under the SSC framework is given in section 2. This is followed in section 3 by the detailed description of the proposed streamline-based semianalytical method under the two-phase flow framework. The two methods are compared directly or indirectly through the SSC inversion results using examples in section 4. The accuracy and speed of the proposed method are demonstrated. Finally, in section 5, we provide further discussion and conclusions.

2 Perturbation Method

Assuming we have measurements of reservoir response $\widehat{\mathbf{d}}(\mathbf{u}, t)$, e.g., pressure or fractional flow rate at producing wells observed at location $\mathbf{u} \in A$ and time t, A is the entire space. The reservoir data $\mathbf{d}$ are nonlinear functions of the parameter vector

$\mathbf{a}$ (e.g., porosity or permeability): $\mathbf{d} = g(\mathbf{a})$. In our case, the function g represents the multiphase flow equations. The inverse problem consists of finding the optimal parameter $\mathbf{a}$ so that the solution $\mathbf{d}(\mathbf{u}, t) = g(\mathbf{a})$ matches the data $\widehat{\mathbf{d}}(\mathbf{u}, t)$, i.e., the mismatch $(\mathbf{d} - \widehat{\mathbf{d}})^2$ is minimized. When a gradient-based method (e.g. steepest descent, Gauss-Newton or conjugate gradient method) is used to find the optimal parameter $\mathbf{a}$, we need to compute the sensitivity coefficient of $\mathbf{d}$, i.e., the derivative of $\mathbf{d}$ with respect to the parameter $\mathbf{a}$.

The simplest way of computing such sensitivity coefficients is the so-called substitution or perturbation method. It computes the first order approximation of the sensitivity coefficient using a finite difference procedure. When adapting the SSC method to find the optimal permeability fields that match the fractional flow rate data $f(w_f, t_f)$, the substitution method can be summarized as follows:

1. Select an initial permeability field, $\mathbf{k}_0 = \{k_0(\mathbf{u}_i), i = 1, ..., N\}$, N being the number of cells in the model.

2. Solve the flow equations for fractional flow rate, $f_0(w_f, t_f)$, at all wells and at all time steps using the initial permeability field. For all master locations $j = 1$, ..., n_m, (taking one at a time and usually $n_m \ll N$), proceed to the following steps:

   - Introduce a small perturbation of permeability $\triangle k_j$ to the initial permeability at master location $\mathbf{u}_j$.

   - Interpolate this small perturbation into the entire field using a selected

interpolating algorithm (SSC uses kriging method). We thus get a perturbation field $\triangle \mathbf{k}_j = \{\triangle k(\mathbf{u}_i), i = 1, ..., N\}$ due to the perturbation at location $\mathbf{u}_j$, $\triangle k_j = \triangle k(\mathbf{u}_j)$.

- Add this perturbation field to the initial permeability field to obtain the updated permeability field $\mathbf{k}' = \mathbf{k}_0 + \triangle \mathbf{k}_j$.
- Solve the flow equations using the updated field $\mathbf{k}'$ to obtain the new fractional flow rate solution, $f'_j(w,t)$ induced by the perturbation at master point $\mathbf{u}_j$.
- The sensitivity coefficient of fractional flow rate with respect to the permeability change at master location $\mathbf{u}_j$ can then be computed as:

$$S_{f,j}(w_f, t_f) = \frac{f'_j(w_f, t_f) - f_0(w_f, t_f)}{\triangle k_j} \tag{4}$$

Thus, for each outer-iteration of the SSC method, a total of $n_m + 1$ flow simulation solutions are needed to obtain all sensitivity coefficients required. This demands much CPU time. In addition, the values of $S_{f,j}(w_f, t_f)$ computed by using this substitution method are sensitive to the magnitude of the introduced perturbation, $\triangle k_j$ if the solution is highly nonlinear to the parameter. More importantly, the substitution method computes sensitivity coefficients of each parameter independently (i.e., one at a time), thus it does not account for joint perturbations, i.e. the spatial relationship, at all n_m master locations. We will show later that this is crucial for achieving good final models.

Many improvements have been proposed to speed up the computation of sensi-

tivity coefficients of fractional flow rate under the finite-difference framework (e.g., Chu et al., 1995; Landa, 1997). Although faster than the perturbation method, these methods all remain computationally intensive and none accounts for joint perturbations.

Xue et al. (1997) used a streamline-based method to solve the flow equations and compute the sensitivity coefficients. Their method speeds up the perturbation approach by taking advantage of the computational speed of streamline-based flow simulation method as compared with a finite-difference method. Although streamline-based flow simulation can be orders of magnitude faster than finite difference, it is still CPU intensive, requiring $n_m + 1$ flow solutions. It shares other shortcomings of the substitution method, i.e., (1) the sensitivity coefficient values depend on the value of $\triangle k_j$ used in the calculation, and (2) it does not account for spatial correlation of perturbations at multiple master locations.

3 Streamline-Based Semi-Analytical Method

We propose a new method for computing sensitivity coefficients based on the streamline algorithm and the analytical relationship between fractional flow rate and the time-of-flight (TOF) of streamlines (Thiele, et al., 1996; Batycky et al., 1997). The TOF is equivalent to the travel time in particle tracking widely used in hydrogeology. The key assumption is that the streamline geometries are insensitive to the relatively small perturbations of the permeability field. This assumption is valid as long as the perturbation is relatively small, which we will show to be the case in the inner

iterations of the SSC. All streamline geometries are then updated after the perturbation in the outer loop of the SSC inversion so that the potential error due to the fixed streamline geometry assumption during the sensitivity coefficient computation could be corrected. The complete set of sensitivity coefficients at all master points are obtained simultaneously (not one at a time as in the perturbation method). The spatial correlation of perturbations at multiple master locations is accounted for by using kriging weights computed from all master locations when propagating the perturbations at master locations to the entire field. The algorithm is developed in detail next. In the streamline-based method, the fractional flow rate for a given producing well w_f at time t_f is expressed as (Batycky et al., 1997):

$$f(w_f, t_f) = \frac{\sum_{s=1}^{n_{w_f}^{sl}} q_s^{sl} f_s^{sl}(t_f)}{\sum_{s=1}^{n_{w_f}^{sl}} q_s^{sl}} \tag{5}$$

where q_s^{sl} is the flow rate associated with streamline s, and $f_s^{sl}(t_f)$ is the fractional flow rate of streamline s at time t_f. $n_{w_f}^{sl}$ is the total number of streamlines arriving to well w_f. The derivative of $f(w_f, t_f)$ with respect to the permeability perturbation at master point j is then:

$$S_{f,j}(w_f, t_f) = \frac{\partial f(w_f, t_f)}{\partial \triangle k_j} = \frac{1}{\sum_{s=1}^{n_{w_f}^{sl}} q_i^{sl}} \sum_{s=1}^{n_{w_f}^{sl}} q_s^{sl} \frac{\partial f_s^{sl}(t_f)}{\partial \triangle k_j} \tag{6}$$

Depending on the flow regime, the fractional flow rate $f_s^{sl}(t_f)$ of streamline s can be expressed as a function of time-of-flight (TOF) τ_s, i.e., $f_s^{sl}(t_f) \sim (\frac{\tau_s}{t_f})$. As an example, the function of $f_s^{sl}(t_f)$ for tracer flow and immiscible two-phase displacement are shown in Figure 1. These functions can either be obtained analytically or numerically.

Assuming the streamline geometry fixed, i.e., the perturbation of permeability only changes the time-of-flight, τ_s along streamline, thus, to compute

$$\frac{\partial f_s^{sl}(t_f)}{\partial \triangle k_j}$$

in (6), we only need to compute

$$\frac{\partial \tau_s}{\partial \triangle k_j}$$

Considering a non-diffusive tracer flow with unit mobility ratio and matched fluid density, we thus have, see Figure 1a:

$$f_s^{sl}(t_f) = \begin{cases} 1, & if\ \tau_s \leq t_f \\ 0, & if\ \tau_s > t_f \end{cases} \tag{7}$$

Since Equation (7) is not differentiable at $\tau_s/t_f = 1$, we use an Error function $Erf(\tau_s/t_f - 1)$ with a small variance to approximate the 1D tracer solution (dashed line in Figure 1a):

$$f_s^{sl}(t_f) \approx 1 - Erf(\frac{\tau_s}{t_f} - 1) \tag{8}$$

hence,

$$\frac{\partial f_s^{sl}(t_f)}{\partial \triangle k_j} = -\frac{1}{t_f} G(\frac{\tau_s}{t_f}) \frac{\partial \tau_s}{\partial \triangle k_j} \tag{9}$$

where

$$G(\frac{\tau_s}{t_f}) = \frac{1}{\sqrt{2\pi}\sigma} e^{-\frac{(\tau_s - t_f)^2}{2t_f^2\sigma^2}}$$

is a Gaussian distribution function with mean 1 and variance σ^2. The variance σ^2 should be small so that the approximation is close to the true function; we will demonstrate later the influence of the variance on the sensitivity coefficients.

Note that, for two-phase immiscible flow, the derivative of fractional flow with respect to time-of-flight can be obtained from the Buckley-Leverett solution (See Figure 1b).

Again, the time-of-flight of streamline s is a function of total flow velocity which is a function of permeability and total pressure along the streamline:

$$\tau_s = \int_0^s \frac{1}{v_s} ds$$

In a discretized numerical model (see Figure 2), the time-of-flight of streamline s from injector to producer is the sum of the time-of-flight in each cell that streamline s passes through, i.e.,

$$\tau_s = \sum_{c=1}^{n_{s,c}} \triangle\tau_{s,c} \tag{10}$$

$n_{s,c}$ being the number of cells crossed by streamline s from injector to producer, and $\triangle\tau_{s,c}$ is the associated time-of-flight for streamline s to pass through cell c.

In Figure (2), for example, the total number of cells crossed by the streamline from injector to producer is 13 (i.e., $n_{s,c} = 13$). Based on the semi-analytical solution (Pollock, 1989), i.e., assuming linear variation of velocity in all directions within a numerical cell, we have:

- if the streamline exits the cell c in the X-direction,

$$\triangle\tau_{s,c} = \triangle\tau_{s,c,x} = \frac{1}{J_x} \ln\left\{\frac{v_{x,0} + J_x(x_e - x_0)}{v_{x,0} + J_x(x_i - x_0)}\right\} \tag{11}$$

- if the streamline exits the cell c in the Y-direction,

$$\triangle\tau_{s,c} = \triangle\tau_{s,c,y} = \frac{1}{J_y}\ln\left\{\frac{v_{y,0} + J_y(y_e - y_0)}{v_{y,0} + J_y(y_i - y_0)}\right\} \tag{12}$$

where

$$J_x = \frac{v_{x,\triangle x} - v_{x,0}}{\triangle x}$$

$$J_y = \frac{v_{y,\triangle y} - v_{y,0}}{\triangle y}$$

$$v_{x,0} = -T_{01}\frac{p_0 - p_1}{\triangle x\phi\mu}, \qquad T_{01} = \frac{2k_0k_1}{k_0 + k_1}$$

$$v_{x,\triangle x} = -T_{02}\frac{p_2 - p_0}{\triangle x\phi\mu}, \qquad T_{02} = \frac{2k_0k_2}{k_0 + k_2}$$

$$v_{y,0} = -T_{03}\frac{p_0 - p_3}{\triangle y\phi\mu}, \qquad T_{03} = \frac{2k_0k_3}{k_0 + k_3} \tag{13}$$

$$v_{y,\triangle y} = -T_{04}\frac{p_4 - p_0}{\triangle y\phi\mu}, \qquad T_{04} = \frac{2k_0k_4}{k_0 + k_4}$$

where $\triangle x$ and $\triangle y$ are the cell size in X and Y directions, ϕ is porosity, μ is viscosity, T_{01} to T_{04} are the transmissibilities for the four interfaces of the cell intersected by the streamline (cell 0 in Figure 2), p_0 to p_4 and k_0 to k_4 are the pressure and permeability values at the current (0) and the surrounding (1 to 4) cells, see Figure 2. (x_i, y_i) and (x_e, y_e) are the inlet and exit coordinates of the streamline in current cell 0, and (x_0, y_0) is the coordinate of the lower-left corner of current cell 0.

From Equations (10) to (13), we have:

$$\frac{\partial \tau_s}{\partial \triangle k_j} = \sum_{c=1}^{n_{s,c}} \left\{ \sum_{g=1}^{4} \frac{\partial \triangle \tau_{s,c}}{\partial T_{0g}} \frac{\partial T_{0g}}{\partial \triangle k_j} + \sum_{l=0}^{4} \frac{\partial \triangle \tau_{s,c}}{\partial p_l} \frac{\partial p_l}{\partial \triangle k_j} \right\} \tag{14}$$

where $\frac{\partial \triangle \tau_{s,c}}{\partial T_{0g}}$ and $\frac{\partial \triangle \tau_{s,c}}{\partial p_l}$ can be computed from Equations (11) and (12), their expressions are given in Appendix. $\frac{\partial p_l}{\partial \triangle k_j}$ are the sensitivity coefficients of pressure with respect to permeability change, their computation is given in the previous paper (Gómez-Hernández et al., 1997; Wen et al., 1998). Finally, from Gómez-Hernández et al., (1997), we have (using harmonic average to compute transmissibility between two cells):

$$\frac{\partial T_{0g}}{\partial \triangle k_j} = \frac{T_{0g}^2}{2} \left\{ \frac{\lambda_j^0}{k_0} + \frac{\lambda_j^g}{k_g} \right\} \tag{15}$$

where λ_j^0 and λ_j^g are the kriging weights attributed to master point j, cells 0 and g (g = 1, ..., 4). Since the kriging weights are computed accounting for all master points, the resulting sensitivity coefficients do account for the spatial rorrelation among all master points, i.e., the permeability perturbations at all master locations are now considered jointly rather that one at a time. The completed set of sensitivity coefficients at all master points are obtained simultaneously. In addition, there is no need to choose a specific value of $\triangle k_j$ before computing sensitivity coefficients.

In summary, the calculation of the sensitivity coefficients, equations (9) and (14) is reduced to a simple book-keeping of streamlines in the simulation model: this is both mathematically simple and computationally fast. The extension of this method to other types of flow (such as immiscible two-phase flow), or to other type of data

(such as distributed saturation), and to 3D, should be straightforward.

It is noted that new streamline geometry is recomputed in each outer iteration of the SSC inversion, i.e., after updating by reruning the simulation. Thus any potential error in sensitivity coefficients by assuming fixed streamline geometry is limited within one iteration, and then self-corrected in the next iteration. The net impact for the SSC inversion is that, for highly heterogeneous model, it may slow down the convergence rate during the inversion and a smaller damping (relaxing) parameter for model updating should be used (see Gómez-Hernández et al., 1997; Wen et al. 1999).

4 Examples

In this section, we compare the accuracy and efficiency of the streamline-based perturbation method and the proposed streamline-based semianalytical method in computing sensitivity coefficients for the SSC inversion.

4.1 Single Master Point

We first compare the sensitivity coefficients with only one master point. Because the perturbation method does not account for the spatial distribution of all master points whereas the proposed method does, the sensitivity coefficient values computed by the two methods are comparable only when there is single master point. Figure 3 provides this comparison: Figure 3a is the 2-D $Ln(k)$ field with constant permeability $Ln(k) = 2$. k has unit of millidarcy (md, 1 md = 9.869×10^{-16} m^2). There are four

producers at the four corners and one water injector at the center of the field: injection rate = 3000 bbl (Barrel)/day (1 bbl = 0.1589873 m^3), assuming unit mobility ratio and matched fluid density, which is equivalent to tracer flow. The production rates are held constant for each producer: 500 bbl/day for wells 1 and 4, 1000 bbl/day for wells 2 and 3. Other reservoir parameters are: thickness $h = 100$ feet, porosity $\phi = 0.2$, viscosity $\mu = 0.3$ cp, and compressibility $c = 10^{-5}$ 1/psi. The streamline geometry for this field is also given in Figure 3a. The fractional flow rate at well 1, $f^0_{w1}(t)$, is shown in Figure 3b.

A single master point is selected close to well 1 with a perturbation of $\triangle(\ln(k))_1 = 0.2$, this perturbation is then propagated through the entire field by kriging to obtain a perturbation field (Figure 3c), resulting in the updated field shown in Figure 3d. An anisotropic variogram with major range in direction 45° is used for this propagation. Next, the flow equation is solved again based on the updated permeability field to obtain the perturbed fractional flow rate $f^1_{w1}(t)$ at well 1 due to the original perturbation at the master point, see Figure 3e. The new streamline geometry for the updated permeability field is also shown in Figure 3d: there is very little change in streamline geometry.

Using the perturbation method, the sensitivity coefficients are computed as:

$$S_f(w_1, t) = \frac{f^1_{w1}(t) - f^0_{w1}(t)}{\triangle k_1}$$

The corresponding values are shown by the solid bullets in Figure 3g. The sensitivity coefficients of pressure for the entire field with respect to the permeability

perturbation at the master point required by the proposed method are shown in Figure 3f, these are computed as part of single phase flow simulation. The solid line in Figure 3g are the results obtained by the proposed method: the results from the two methods are quite close. This indicates the accuracy of the proposed method.

As mentioned previously, the sensitivity coefficients computed by the perturbation method are sensitive to the magnitude of the perturbation $\triangle k$ used in the calculation. Figure 4 shows the sensitivity coefficients at well 1 using different perturbation values for $\triangle k$ at the master point. A 10 % perturbation of the initial value provides reasonably stable results. Considering the fact that the appropriate $\triangle k$ will change for different master points and at different wells because of their relative configurations, the accuracy of sensitivity coefficients using the perturbation method will vary for different master points and for different wells by using the same $\triangle k$ value.

As for the proposed method, an Error function is used to approximate the analytical 1D tracer flow solution, see Figure 1a. The derivative of the Error function is a Gaussian function. The values of sensitivity coefficient using the proposed method will be influenced by the selected variance value used in the Gaussian function. This is shown in Figure 5 using the same field as shown in Figure 3. The larger this variance value, the smoother the sensitivity coefficient results. Therefore the variance should be small, and the results are quite stable with range of 0.01-0.001. Note that the accuracy of the sensitivity coefficients calculated at different master points and for different wells does not change if we use the same variance value.

Our experience has been that the positive or negative signs of the sensitivity

coefficients, which guide the direction of perturbation in the optimization, as well as the relative values at different locations are more important than their absolute values for the SSC inversion.

4.2 Multiple Master Points

For the case of multiple master points, the sensitivity coefficients calculated by the two methods are not directly comparable since the proposed method accounts for the spatial correlation of perturbations at the multiple master points whereas the perturbation method does not. Nevertheless, we can judge their accuracy indirectly by comparing the final inversion results and the behavior of the corresponding objective functions.

Figure 6 shows a 2-D geostatistical reference field (50×50 grid with cell size 80 feet $\times$ 80 feet) and the corresponding fractional flow rate data at 4 wells. The reference field is generated by using the Sequential Gaussian Simulation (Deutsch and Journel, 1998). The main features observed from this field are: (1) a high permeability zone and a low permeability zone in the middle of the field, (2) high interconnectivity between wells W5 and W3, and (3) low interconnectivity between wells W5 and W4. These features are the main characterics when comparing results from different methods in this example. The injection rate at the central well (W5) is 1600 bbl/day, and the production rate for the 4 producing wells (W1 to W4) is 400 bbl/day/well. Fractional flow rates at 4 producing wells are computed with streamline simulation. All other flow parameters (thickness, porosity and viscosity) used in the simulation

are the same as in the previous example. 1000 streamlines are used in this streamline simulation. The SSC method is then used to construct permeability realizations matching the fractional flow rate data at the 4 producing wells. No pressure data is used in this example. Initial unconditional realizations required by the SSC are generated using the same method with the same parameters (histogram and variogram) as used to generate the reference model.

Figure 7 shows three initial permeability fields (top row) and the resulting fields updated by SSC using the two different methods for computing sensitivity coefficients (second row: perturbation method, third row: proposed method). The bottom row shows the decreases of the objective function with number of iterations. The same 25 randomly selected master points are used for all realizations.

From this figure, we can see that, visually, the proposed method provides more accurate permeability fields with lower objective function and with representation of spatial variation patterns closer to the reference field. Also, using the proposed method, the objective function behaves better during the inversion process, i.e., the objective function decreases monotonically, whereas, using the perturbation method, the value of objective function fluctuates.

The comparison of individual realizations as shown in Figure 7 is somewhat difficult. A better comparison of the inverse results from the two methods is given by the ensemble results calculated from 200 realizations, see Figure 8. The ensemble average field provides information about common large scale variation patterns among different realizations, while the standard deviation field displays the degree of variation

(uncertainty) among realizations.

Comparing with the reference field given at the bottom of the figure, the inverse results using the proposed method are clearly superior in that the results (1) better reproduce the reference spatial patterns and are thus more accurate, and (2) have smaller standard deviations and are thus less uncertain.

In summary, compared to the perturbation method, the inverse results from the proposed method in the SSC inversion have the following characteristics:

- better behavior of objective function: monotonically decreasing for almost all realizations,
- lower objective function,
- better reproduction of the reference spatial patterns with less uncertainty.

These indirectly indicate that the proposed method provide more accurate sensitivity coefficients that are better suited for the SSC inversion.

4.3 CPU Time Comparison

The computational efficiency of the proposed method is now compared with the perturbation method. The CPU time for computing sensitivity coefficients of fractional flow rate using the two methods depends mainly on the following three parameters:

1. size of the simulation model (number of cells),
2. number of master points, and

3. total number of streamlines used.

Other minor factors include (1) the number of producers and (2) the number of time steps in the simulation. Among these factors, the model size is the dominant factor due to the flow simulation.

Figure 9 shows CPU time (SGI Indigo workstation) of 10 SSC iterations versus the number of cells in the model with 25 master points and 1000 streamlines. The number of streamlines required for the simulation is problem dependent. In general, we can try different number of streamlines until obtaining stable simulation results.

From Figure 9, we can see that, for a small (e.g. 25×25) model, the perturbation method is slightly faster than the proposed method because solving a few flow equations using the streamline method is quicker than the proposed book-keeping of streamlines. The book-keeping of streamline includes (1) all intersections of each streamline with grid cells, (2) TOF of each streamline across each cell, (3) integration of all required information according to Equations (9) and (14) to get sensitivity coefficients for all master points. As the model becomes larger, the CPU time increases dramatically using the perturbation method because the flow equations must be solved many more times (total number of flow simulation = iteration number $\times$ (number of master points + 1) for the perturbation method). Whereas the CPU time for the proposed method increases much more slowly than the perturbation method (total number of flow simulation = iteration number for the proposed method). With a 100×100 grid model, the CPU time using the perturbation method is more than 5 times that using the proposed method.

Other non-SSC based methods for inverting production data that require flow simulations at every iteration for every cell or zone (i.e., full matrix) without using streamline-based simulator could be orders of magnitude slower than the proposed method (e.g., Chu et al., 1995; He et al., 1996; Landa, 1997). The CPU time of one such inversion is also given in Figure 9 for comparison. Note that the full matrix based direct method used can not run model with cells number larger than 30×30 due to its extreme memory demanding.

5 Summary and Discussion

We have presented a new methodology for computing sensitivity coefficients of fractional flow rate with respect to permeability, based on an analytical solution from streamlines. This method has been implemented within the SSC framework for inverting permeability models from fractional flow rate data. We have verified the proposed method by comparing the sensitivity coefficient results using the perturbation method for only one master point. For multiple master points, we have demonstrated that the proposed method is more accurate and better suited for the SSC inversion than the perturbation method. The SSC inversion with the proposed method provides a better inverse permeability field with a lower objective function, less uncertainty, and better spatial variation patterns than with the perturbation method. We have also shown that the proposed method is computationally more efficient than the perturbation method.

The proposed streamline-based method of sensitivity coefficient calculation has

the following characteristics:

- The fractional flow rate is the sum of fractional flow rate of all contributing streamlines, see equation (5).
- The sensitivity coefficient of fractional flow rate for each streamline is a function of sensitivity of time-of-flight and a derivative of the 1D solution, see equation (9).
- The sensitivity coefficient of time-of-flight is separated into a pressure part and a permeability part along the streamline, see equation (14).
- The pressure part is computed directly from a single-phase flow solution, (see Gómez-Hernández et al., 1997 and Wen et al., 1998).
- The permeability part comes from the same kriging algorithm that is used to propagate the permeability perturbation, see equation (15).
- The derivatives of time-of-flight with respect to transmissibility and pressure are obtained from the analytical expression of time-of-flight, see Appendix.

The computation of sensitivity coefficients with respect to permeability perturbation is reduced to solving a single-phase flow equation only **once** and then keeping track of the streamlines from injectors to producers. The completed set of sensitivity coefficients at all master locations are obtained simultaneously, and the spatial correlation of perturbations at multiple master locations is accounted for. It is fast and more accurate than the perturbation method.

We believe that the improved accuracy of the proposed method results are due to the following reasons:

- It jointly accounts for the perturbations of multiple master locations through the kriging weights. Thus the spatial correlation of perturbation values among all master points is intrinsically built in. Accounting such spatial correlation is essential in the SSC inversion, while the traditional perturbation method can not build in such important spatial correlation.

- It does not depend on the magnitude of the specific perturbation values.

- The absolute values of the sensitivity coefficients are not as important to the inversion as their relative values at different locations, as well as their positive or negative sign for the SSC inversion.

- The assumption that streamline geometry is relatively insensitive to the permeability perturbation within a single inner iteration of the SSC does not limit the application of the proposed method due to the updating of streamlines after each outer loop of SSC inversion. Also, this assumption is reasonable as long as the permeability perturbation is small, which is the case within each inner iteration.

The proposed method requires the sensitivity coefficients of single-phase pressure to the permeability change for all cells intersected by streamlines and their surrounding cells (essentially all cells of the model). We take advantage of the earlier method

of computing sensitivity coefficients of pressure for all simulation cells within a single-phase flow simulation (Gómez-Hernández et al., 1997; Wen et al., 1998).

In this paper, we have used tracer flow to represent an unit mobility ratio and matched fluid density displacement, for which the exact 1D analytical solution along the streamline is available and the pressure field does not change during the course of injection. For other flow regimes or boundary conditions, e.g. with nonunit mobility ratio and different fluid densities, with changes in well configuration, or with changes in injection or production well rates, the pressure field and the streamline geometries would have to be updated within any one flow simulation (Batycky et al., 1997). In such cases, we need to retain all information about the locations and geometries of all streamlines and their associated time-of-flight, as well as the associated pressure fields. When the analytical 1D solution along the streamline is not available, other methods, e.g. semi-analytical or numerical methods can be used to compute the 1D fractional flow rate solution. We may then obtain nonsmooth 1D solutions which would require smoothing, so that they are differentiable.

This paper presented only the sensitivity coefficients of fractional flow rate to permeability. The same method can easily be extended to compute sensitivity coefficients of fractional flow to porosity or sensitivity coefficients of saturation at any locations that might be available from well data or even 4D seismic in the future. In future papers, we will show results for more complex reservoir examples and additional boundary conditions.

Finally, it is noted that the proposed method is directly applicable to intergrate

tracer test data for aquifer formation characterization in hydrogeology.

Acknowledgement

We thank Prof. J. J. Gómez-Hernández and Prof. J. E. Capilla, Technical University of Valencia, for their support and discussions on the SSC inversion. Special thanks are due to Prof. Andre G. Journel, Stanford University, for his careful review and suggestions for this manuscript.

References

Batycky, R. P., Blunt, M. J., and Thiele, M. R., 1997. A 3D field-scale streamline-based reservoir simulator. *SPE Reservoir Engineering*, November:246-254.

Capilla, J. E., Gómez-Hernández, J. J., and Sahuquillo, A., 1997. Stochastic simulation of transmissivity fields conditioning to both transmissivity and piezometric data, 2. demonstration in a synthetic case. *Journal of Hydrology*, 203(1-4), 175-188.

Chu, L., Reynolds, A. C., and Oliver, D, S., 1995. Computation of sensitivity coefficients for conditioning the permeability field to well-test pressure data. *In Situ*, 19(2):179-223.

Deutsch, C. V. and Journel, A. G., 1998. *GSLIB: Geostatistical Software Library and User's Guide*. Second Edition, Oxford University Press, New York, 369pp.

Gómez-Hernández J. J. and Journel, A. G., 1993. Joint sequential simulation of multi-Gaussian fields. In A. Soares, editor, *Geostatistics Troia 1992*, volume 1, pages 85–94. Kluwer.

Gómez-Hernández, J. J., Sahuquillo, A., and Capilla, J. E., 1997. Stochastic simulation of transmissivity fields conditional to both transmissivity and piezometric data, 1. The theory. *J. of Hydrology*, 203(1-4), 162-174.

He, N., Reynolds, A. C., and Oliver, D. S., 1996. Three-dimensional reservoir description from multiwell pressure data and prior information. In *1996 SPE Annual Technical Conference and Exhibition Formation Evaluation and Reservoir Geology*, pages 151–166, Denver, CO, October 1996. Society of Petroleum Engineers. Paper Number 36509.

Hu, L. Y., Blanc, G., and Noetinger, B., 1999. Gradual deformation and iterative calibration of sequential stochastic simulations. In *Proceedings of IAMG'99*, S. Lippard, A. Nassvol and R. Sinding-Larsen (eds.), Trondheim, Norway.

Journel, A. G., 1989. *Fundamentals of Geostatistics in Five Lessons.* Volume 8 Short Course in Geology. American Geophysical Union, Washington, D.C.

Landa, J. L., 1997. *Reservoir Parameter Estimation Constrained to Pressure Transients, Performance History and Distributed Saturation Data.* PhD thesis, Stanford University, Stanford.

Oliver, D. S., 1996. Multiple realizations of the permeability field from well test data. *SPEJ*, 1(2):145–154.

Pollock, D. W., 1989. Documentation of computer programs to compute and dis-

play pathline results from the US geological servey modular three-dimensional finite-difference ground-water flow model. Technical Report Open File Report 89-381, U.S. Geological Survey.

Sun, N-Z., 1994. *Inverse Problems in Groundwater Modeling.* Kluwer Academic Publishers, Boston, 337pp.

Tarantola, A., 1987. *Inverse Problem Theory: Methods for Data Fitting and Model Parameter Estimation.* Elsevier, Amsterdam, The Netherlands, 613pp.

Thiele, M. R., Batycky, R. P., Blunt, M. J., and Orr F. M. Jr., 1996. Simulating flow in heterogeneous systems using streamtubes and streamlines. *SPE Reservoir Engineering*, Feb., 5-12.

Tjelmeland, H., 1997. A note on the Bayesian approach to history matching of reservoir characteristics. In V. Pawlowsky, editor, *3rd Annual Conference of International Asso. for Mathematical Geology*, pages Part II, 773–777, Barcelona, Spain, 22-27, Sept. 1997.

Wen, X.-H., 1996. *Stochastic Simulation of Groundwater Flow and Mass Transport in Heterogeneous Aquifers: Conditioning and Problem of Scales.* PhD thesis, Polytechnic University of Valencia, Valencia, Spain.

Wen, X.-H., Gómez-Hernández, J. J., Capilla, J. E., and Sahuquillo, A., 1996. The significance of conditioning on piezometric head data for predictions of mass transport in groundwater modeling. *Math. Geology*, 28(7):961–968.

Wen, X.-H., Deutsch, C. V., and Cullick, A. S., 1998. High resolution reservoir models integrating multiple-well production data. *SPE Journal*, December, 344-355.

Wen, X.-H., Capilla, J. E., Deutsch, C. V., Gómez-Hernández, J. J., and Cullick, A. S., 1999. A program to create permeability field that honor single phase flow rate and pressure data. *Computers & Geosciences*, 25, 217-230.

Wen, X.-H., Tran, T. T., Behrens, R. A., and Gómez-Hernández, J. J., 2000. Production data integration in sand/shale reservoirs using sequential self-calibration and geomorphing: A comparison. In *2000 SPE Annual Technical Conference and Exhibition*, Dallas, Texas, 1-4, October 2000, SPE paper number 63063.

Xu, W., Tran, T. T., Srivastava, R. M., and Journel, A. G., 1992. ntegrating seismic data in reservoir modeling: the collocated cokriging alternative. SPE Paper Number 24742, 1992.

Xue, G. and Datta-Gupta, A., 1997. Structure preserving inversion: An effective

approach to conditioning stochastic reservoir models to dynamic data. In *1997 SPE Annual Technical Conference and Exhibition Formation Evaluation and Reservoir Geology*, pages part II, 101–113, San Antonio, TX, October 1997.

Yeh, W. W-G., 1986. Review of parameter identification procedures in groundwater hydrology: The inverse problem. *Water Resources Research*, 22(2):95–108.

Zhu, H and A. G. Journel, A. G., 1993. Formatting and integrating soft data: Stochastic imaging via the Markov-Bayes algorithm. In A. Soares, editor, *Geostatistics Troia 1992*, volume 1, pages 1–12. Kluwer.

Appendix: Derivation of Time-of-Flight Derivatives

From Equations (11) to (13), we have:

$$\triangle\tau_{s,c,x} = \frac{-\triangle x^2\phi\mu}{A_x}\ln\left\{\frac{\triangle xT_{01}(p_0-p_1)+A_x(x_e-x_0)}{\triangle xT_{01}(p_0-p_1)+A_x(x_i-x_0)}\right\}$$

$$\triangle\tau_{s,c,y} = \frac{-\triangle y^2\phi\mu}{A_y}\ln\left\{\frac{\triangle yT_{03}(p_0-p_3)+A_y(y_e-y_0)}{\triangle yT_{03}(p_0-p_3)+A_y(y_i-y_0)}\right\}$$

where $A_x = T_{01}(p_1-p_0)+T_{02}(p_2-p_0)$, and $A_y = T_{03}(p_3-p_0)+T_{04}(p_4-p_0)$.

The derivatives required in Equation (14) are the following (ref. to Figure 2):

$$\frac{\partial\triangle\tau_{s,c,x}}{\partial T_{01}} = \frac{-\triangle x^2\phi\mu(p_0-p_1)}{A_x^2}\left\{\ln\frac{D_x}{C_x}+A_x\frac{[\triangle x-(x_e-x_0)]\,C_x-[\triangle x-(x_i-x_0)]\,D_x}{C_xD_x}\right\}$$

$$\frac{\partial\triangle\tau_{s,c,x}}{\partial T_{02}} = \frac{-\triangle x^2\phi\mu(p_0-p_2)}{A_x^2}\left\{\ln\frac{D_x}{C_x}+A_x\frac{-(x_e-x_0)C_x+(x_i-x_0)D_x}{C_xD_x}\right\}$$

$$\frac{\partial\triangle\tau_{s,c,x}}{\partial T_{03}} = \frac{\partial\triangle\tau_{i,s,x}}{\partial T_{04}} = 0$$

$$\frac{\partial\triangle\tau_{s,c,x}}{\partial p_0} = \frac{-\triangle x^2\phi\mu}{A_x^2}\left\{(T_{01}+T_{02})\ln\left(\frac{D_x}{C_x}\right)+\right.$$

$$\left.A_x\frac{[\triangle xT_{01}-(T_{01}+T_{02})(x_e-x_0)]\,C_x-[\triangle xT_{01}-(T_{01}+T_{02})(x_i-x_0)]\,D_x}{C_xD_x}\right\}$$

$$\frac{\partial \triangle \tau_{s,c,x}}{\partial p_1} = \frac{- \triangle x^2 \phi \mu}{A_x^2} \left\{ -T_{01} \ln \left(\frac{D_x}{C_x} \right) +$$

$$A_x \frac{[- \triangle x T_{01} + T_{01}(x_e - x_0)] C_x - [- \triangle x T_{01} + T_{01}(x_i - x_0)] D_x}{C_x D_x} \right\}$$

$$\frac{\partial \triangle \tau_{s,c,x}}{\partial p_2} = \frac{- \triangle x^2 \phi \mu}{A_x^2} \left\{ -T_{02} \ln \left(\frac{D_x}{C_x} \right) + A_x \frac{T_{02}(x_e - x_0) C_x - T_{02}(x_i - x_0) D_x}{C_x D_x} \right\}$$

$$\frac{\partial \triangle \tau_{s,c,x}}{\partial p_3} = \frac{\partial \triangle \tau_{i,s,x}}{\partial p_4} = 0$$

where $C_x = \triangle x T_{01}(p_0 - p_1) + A_x(x_i - x_0)$ and $D_x = \triangle x T_{01}(p_0 - p_1) + A_x(x_e - x_0)$.

Similarly,

$$\frac{\partial \triangle \tau_{s,c,y}}{\partial T_{03}} = \frac{- \triangle y^2 \phi \mu (p_0 - p_3)}{A_y^2} \left\{ \ln \frac{D_y}{C_y} + A_y \frac{[\triangle y - (y_e - y_0)] C_y - [\triangle y - (y_i - y_0)] D_y}{C_y D_y} \right\}$$

$$\frac{\partial \triangle \tau_{s,c,y}}{\partial T_{04}} = \frac{- \triangle y^2 \phi \mu (p_0 - p_4)}{A_y^2} \left\{ \ln \frac{D_y}{C_y} + A_y \frac{-(y_e - y_0) C_y + (y_i - y_0) D_y}{C_y D_y} \right\}$$

$$\frac{\partial \triangle \tau_{s,c,y}}{\partial T_{01}} = \frac{\partial \triangle \tau_{s,c,y}}{\partial T_{02}} = 0$$

$$\frac{\partial \triangle \tau_{s,c,y}}{\partial p_0} = \frac{- \triangle y^2 \phi \mu}{A_y^2} \left\{ (T_{03} + T_{04}) \ln \left(\frac{D_y}{C_y} \right) +$$

$$A_y \frac{[\triangle y T_{03} - (T_{03} + T_{04})(y_e - y_0)]\, C_y - [\triangle y T_{03} - (T_{03} + T_{04})(y_i - y_0)]\, D_y}{C_y D_y} \Bigg\}$$

$$\frac{\partial \triangle \tau_{s,c,y}}{\partial p_3} = \frac{- \triangle y^2 \phi \mu}{A_y^2} \left\{ -T_{03} \ln \left(\frac{D_y}{C_y} \right) + \right.$$

$$A_y \frac{[- \triangle y T_{03} + T_{03}(y_e - y_0)]\, C_y - [- \triangle y T_{03} + T_{03}(y_i - y_0)]\, D_y}{C_y D_y} \Bigg\}$$

$$\frac{\partial \triangle \tau_{s,c,y}}{\partial p_4} = \frac{- \triangle y^2 \phi \mu}{A_y^2} \left\{ -T_{04} \ln \left(\frac{D_y}{C_y} \right) + A_y \frac{T_{04}(y_e - y_0) C_y - T_{04}(y_i - y_0) D_y}{C_y D_y} \right\}$$

$$\frac{\partial \triangle \tau_{s,c,y}}{\partial p_1} = \frac{\partial \triangle \tau_{s,c,y}}{\partial p_2} = 0$$

where $C_y = \triangle y T_{03}(p_0 - p_3) + A_y(y_i - y_0)$ and $D_y = \triangle y T_{03}(p_0 - p_3) + A_y(y_e - y_0)$.

Figure Captions

Figure 1: (a) Analytical 1D solution of tracer flow and its approximation using a Gaussian cumulative function (dashed line), and (b) analytical 1D Buckley-Leverett solution of two-phase immiscible displacement.

Figure 2: Schematic illustration of tracking a streamline through a discretized numerical model.

Figure 3: Comparison of sensitivity coefficients computed by the two methods for the case of a single master point.

Figure 4: Sensitivity coefficients computed by the perturbation method using different perturbation values at the master point.

Figure 5: Sensitivity coefficients computed by the proposed method using different variance values to approximate the 1D analytical solution.

Figure 6: A synthetic geostatistical reference field and the fractional flow rate data from the four corner wells.

Figure 7: Three realizations of initial (top row) and inverse results from the SSC method using the perturbation (second row) and the proposal (third row) methods for computing sensitivity coefficients, and the variations of objective functions after each iteration (bottom row).

Figure 8: Ensemble fields (average and standard deviation) from 200 inverted realizations using the two methods for computing sensitivity coefficients.

Figure 9: Comparison of CPU times for 10 SSC iterations using the two methods of computing sensitivity coefficients, as well as the CPU time for one full matrix (non-ssc) based direct method.

Figures

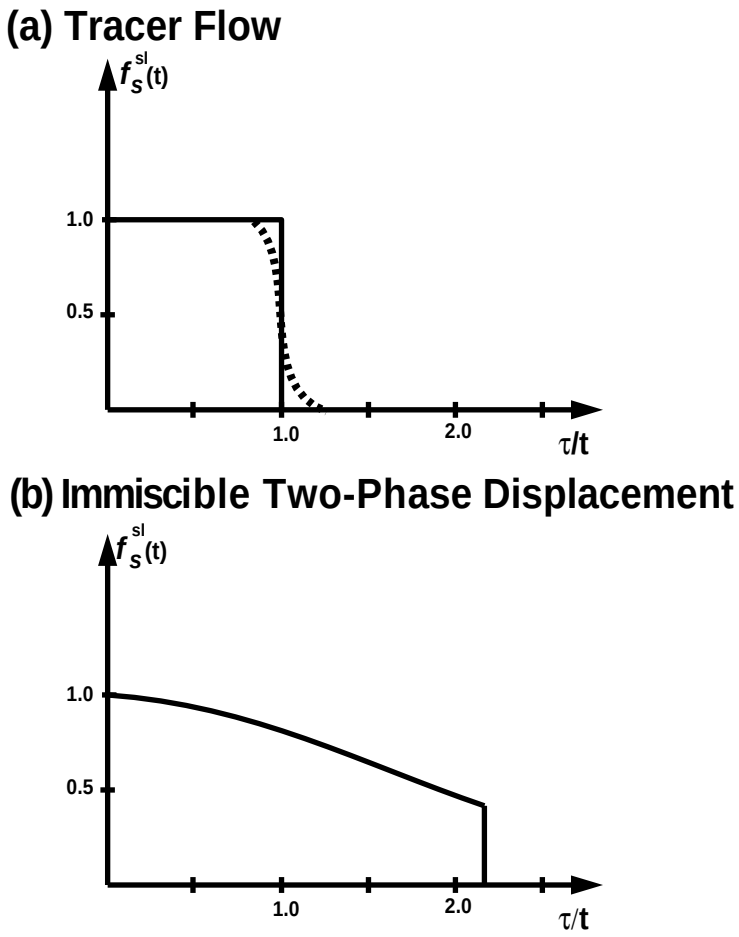

Figure 1: (a) Analytical 1D solution of tracer flow and its approximation using a Gaussian cumulative function (dashed line), and (b) analytical 1D Buckley-Leverett solution of two-phase immiscible displacement.

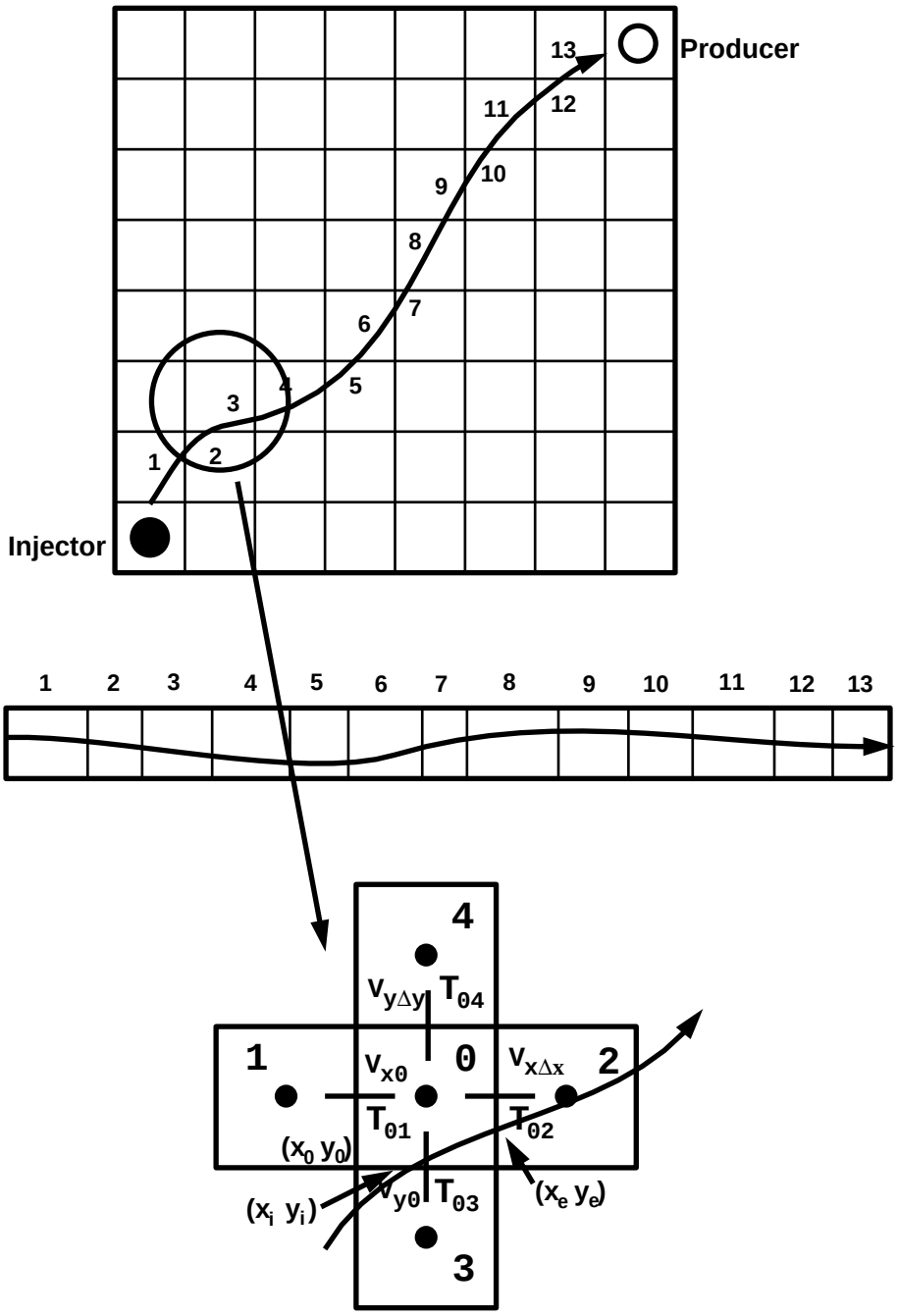

Figure 2: Schematic illustration of tracking a streamline through a discretized numerical model.

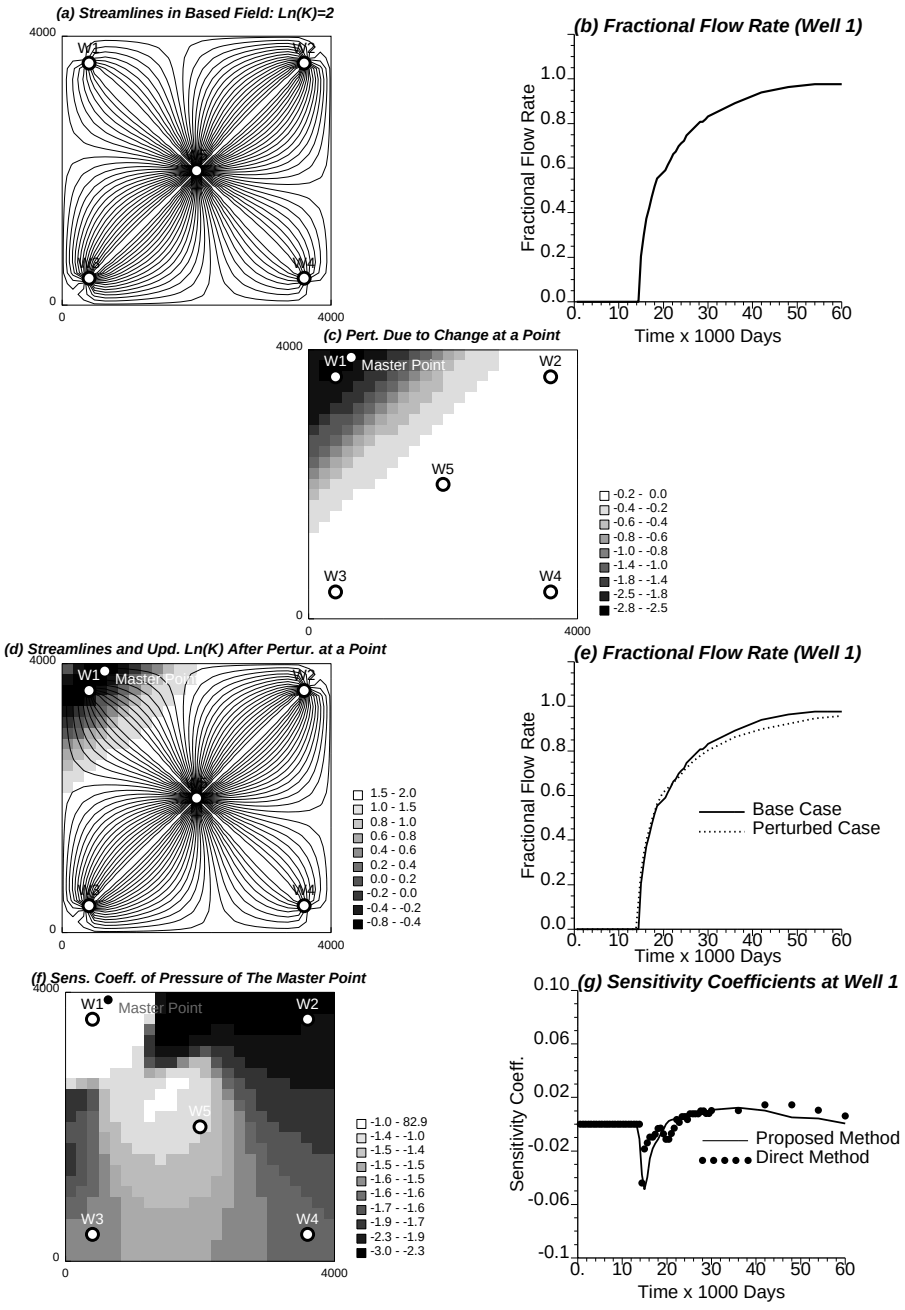

Figure 3: Comparison of sensitivity coefficients computed by the two methods for the case of a single master point.

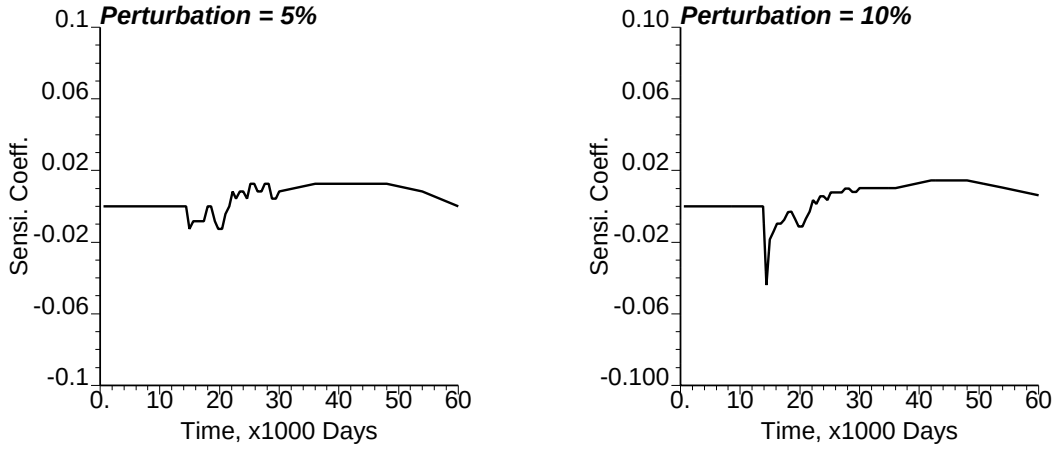

Figure 4: Sensitivity coefficients computed by the perturbation method using different perturbation values at the master point.

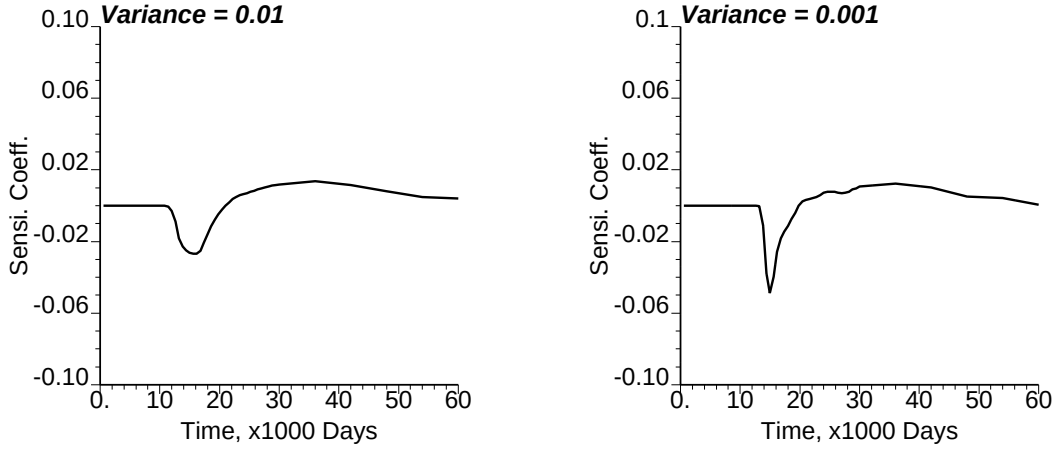

Figure 5: Sensitivity coefficients computed by the proposed method using different variance values to approximate the 1D analytical solution.

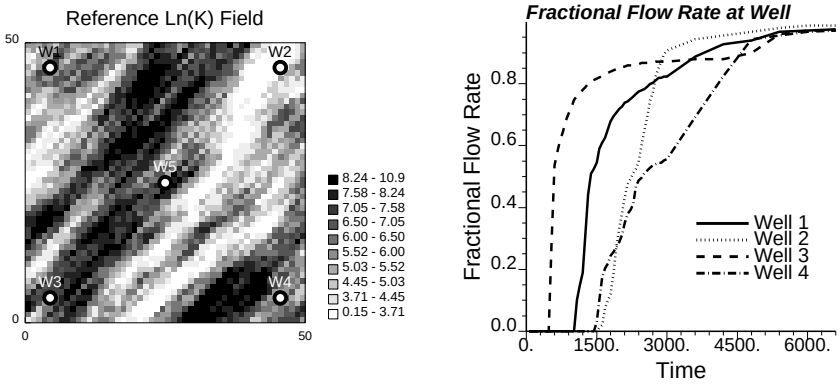

Figure 6: A synthetic geostatistical reference field and the fractional flow rate data from the four corner wells.

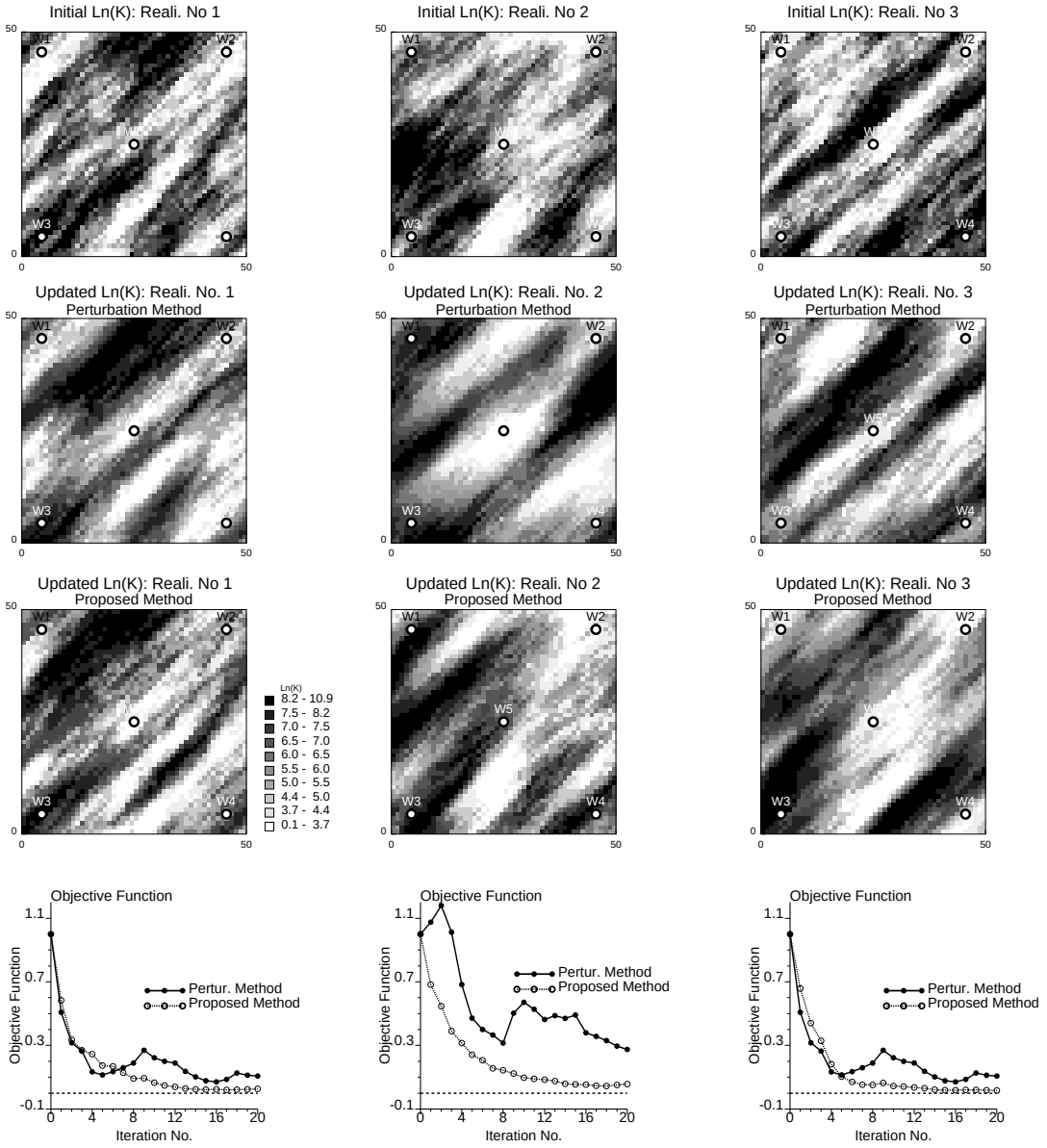

Figure 7: Three realizations of initial (top row) and inverse results from the SSC method using the perturbation (second row) and the proposal (third row) methods for computing sensitivity coefficients, and the variations of objective functions after each iteration (bottom row).

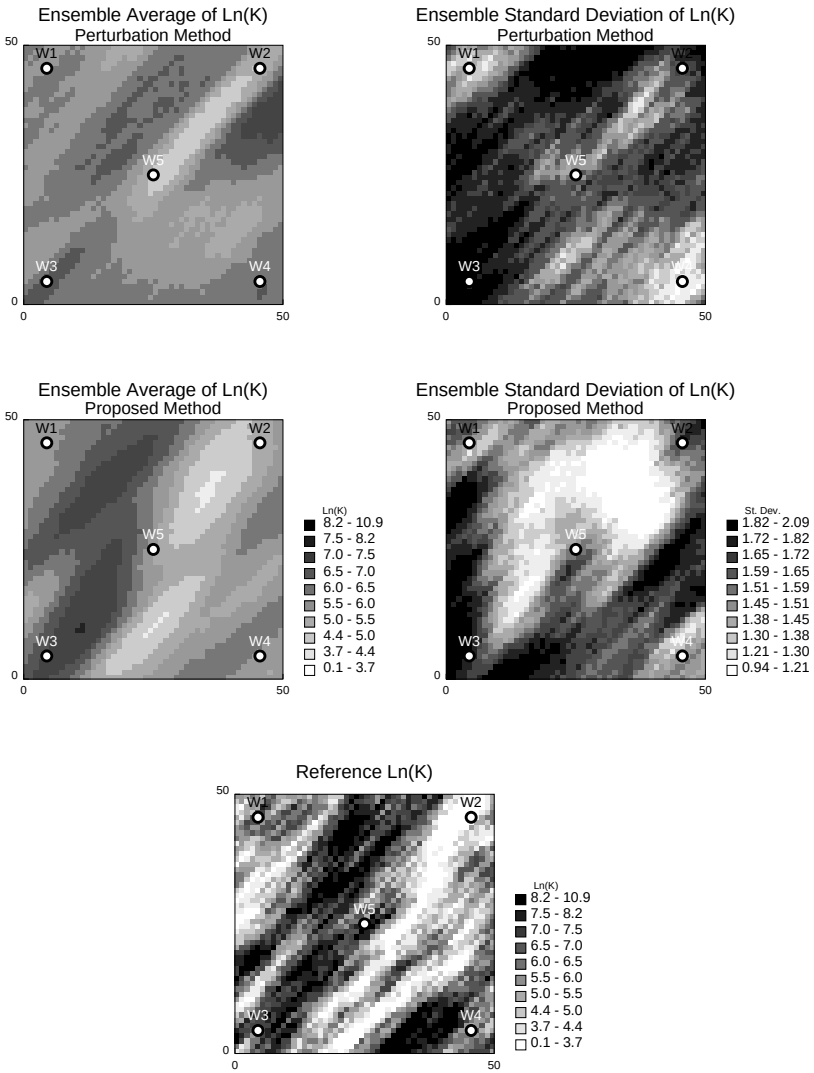

Figure 8: Ensemble fields (mean and standard deviation) from 200 inverted realizations using the two methods for computing sensitivity coefficients.

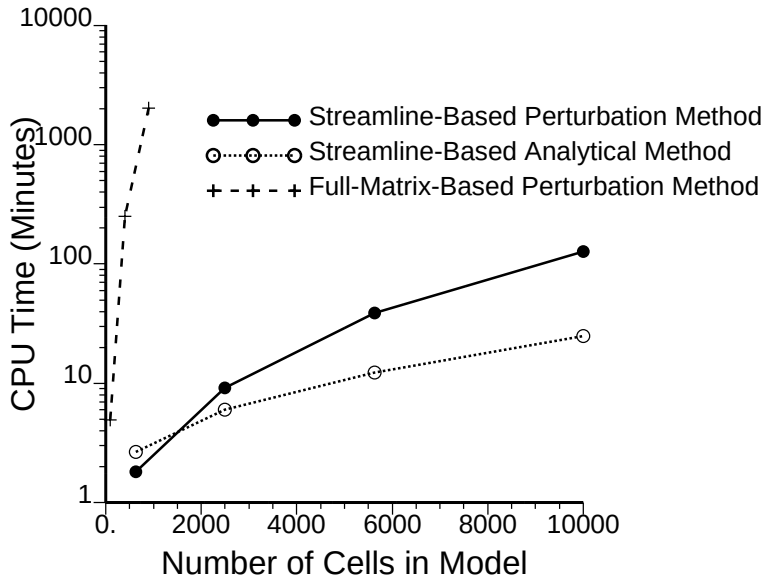

Figure 9: Comparison of CPU times for 10 SSC iterations using the two methods of computing sensitivity coefficients, as well as the CPU time for one full matrix (non-ssc) based direct method.